Noncollinear magnetic structure of MnTe$_2$

P. Burlet and E. Ressouche

Département de Recherche Fondamentale sur la Matière Condensée, SPSMS-MDN, CEA/Grenoble,
17 rue des Martyrs, 38054 Grenoble Cédex 9, France

B. Malaman and R. Welter

Laboratoire de Chimie du solide minéral associé au CNRS, Université Henri Poincaré, Nancy I, Boîte Postale 239, 54506 Vandoeuvre
les Nancy Cédex, France

J. P. Sanchez and P. Vulliet

Département de Recherche Fondamentale sur la Matière Condensée, SPSMS-MRS, CEA/Grenoble,
17 rue des Martyrs, 38054 Grenoble Cédex 9, France

The crystallographic and magnetic properties of the MnTe$_2$ compound have been investigated by ^{125}Te Mössbauer spectroscopy and by neutron diffraction on both powder and single-crystal samples. From T_N down to 4.2 K, the single-crystal experiment, performed in an external magnetic field up to $H=4$ T, strongly supports the conclusion that the magnetic structure is noncollinear with the magnetic moments of the four manganese ions of the unit cell pointing along the body diagonals of the cube ($\mu_{Mn}\|\langle 111\rangle$) which correspond to their local axes, as shown from Mössbauer spectroscopy. [S0163-1829(97)07145-2]

I. INTRODUCTION

The MnTe$_2$ semiconductor compound crystallizes with the pyrite-type structure (space group $Pa3$, $a=6.943$ Å at room temperature, Fig. 1). The manganese atoms occupy the $(4a)$ site $(0,0,0)$, while the tellurium ones are located in a $(8c)$ position (x_{Te},x_{Te},x_{Te}). Each cation Mn^{2+} is sixfold coordinated by distorted octahedra of Te atoms. The point-group symmetry of the manganese ions is $3/m$ and the local axis of each of them is along a particular $\langle 111\rangle$ direction of the cubic lattice (Table I). This compound undergoes a second-order antiferromagnetic transition at $T_N\approx 86.5$ K. The nature of its magnetic structure has been subject to controversy.[1-3] A first neutron-diffraction investigation, performed on a polycrystalline sample,[1] was interpreted in terms of a well known type-I antiferromagnetic structure with a

$(+ -)$ sequence of ferromagnetic (001) planes, the magnetic moments being in the plane [Fig. 2(a) and Table I]. This model turned out to be in contradiction with further Mössbauer experiments.[2] A noncollinear magnetic structure, was then proposed.[3] At temperatures immediately below T_N, the magnetic moments of the four manganese ions of the unit cell point along different body diagonals of the cube ($\mu_{Mn}\|\langle 111\rangle$) corresponding to their local axes [Fig. 2(c) and Table I]. More recent Mössbauer results are consistent with the occurrence of a spin reorientation below 60 K which was ascribed to an increase of the x_{Te} parameter as temperature decreases.[4] The low-temperature data are best described assuming a noncollinear magnetic structure in which the Mn^{2+} moments are along a diagonal of the (001) planes ($\mu_{Mn}\|\langle 110\rangle$) [Fig. 2(b) and Table I]. Both models (a) and (b) imply domains in the cubic $Pa3$ space group, whereas model (c) is single domain. It should be noted that the neutron-diffraction technique, neither on a powder sample, nor on a multidomain single crystal, is able to distinguish
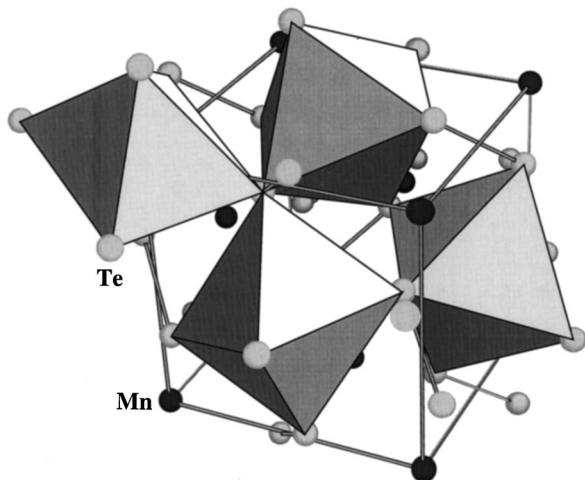
FIG. 1. Crystallographic structure.

TABLE I. The different proposed magnetic models compatible with powder neutron diffraction. Models (a) and (b), respectively, give six and three domains deduced by rotation around the [111] axis and the perpendicular mirror plane. Model (c) is invariant over the symmetry operations of the space group and then no domain exists.

Manganese position	Local axis of symmetry	Model (a) moment	Model (b) moment	Model (c) moment
(0 0 0)	$[111]$	$[m_1 m_2 0]$	$[mm0]$	$[mmm]$
(1/2, 1/2, 0)	$[1\bar{1}\bar{1}]$	$[m_1 m_2 0]$	$[m m \bar{0}]$	$[m m \bar{m}]$
(0, 1/2, 1/2)	$[\bar{1}1\bar{1}]$	$[\bar{m_1} \bar{m_2} 0]$	$[\bar{m} m 0]$	$[\bar{m} m m]$
(1/2, 0, 1/2)	$[\bar{1}\bar{1}1]$	$[\bar{m_1} \bar{m_2} 0]$	$[\bar{m} \bar{m} 0]$	$[\bar{m} \bar{m} m]$

Model (a)
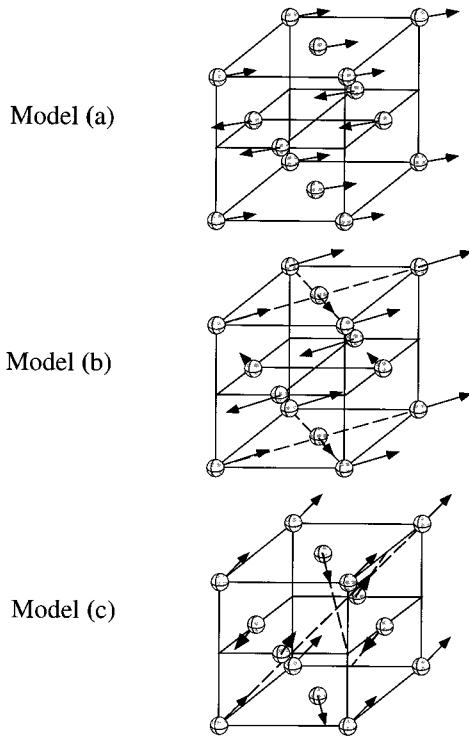
Model (b)

Model (c)

FIG. 2. The different models of magnetic structures.

between these models. Such a differentiation requires a constraint to be applied while cooling the sample, such as an external magnetic field.

In the literature, one often encounters the terminology single-$\mathbf{k}$, double-$\mathbf{k}$, and triple-$\mathbf{k}$ for these three models. This terminology is abusive in the case of $MnTe_2$ from a formal point of view, since it refers to a pseudo-face-centered-cubic lattice occupied by the manganese atoms and to a description of the structure in terms of a propagation vector $\mathbf{k} = (100)$. This description is not true in the primitive cubic lattice $Pa3$ since, in this space group, (100) is a reciprocal-lattice vector and therefore does not lie in the first Brillouin zone. The structure corresponding to the observed additional peaks has a propagation vector $\mathbf{k}=0$, and one actually has to take into account a site with four Bravais sublattices.

In order to obtain more information on the magnetic structure of $MnTe_2$, and on the possible spin reorientation at 60 K, we have performed a set of Mössbauer investigations as well as neutron experiments on a powder sample and on a single crystal in zero and under an applied magnetic field.

II. SAMPLE PREPARATION AND EXPERIMENTAL METHODS

$MnTe_2$ was prepared from commercially available high-purity elements: Mn (powder, 99.9%), and Te (pieces, 99.999%). A pellet of stoichiometric mixture was compacted using a steel die and then introduced into silica tubes sealed under argon (300 mm Hg). Preliminary homogenization treatment was conducted at 773 K. The sample was then annealed for 2 weeks at 873 K. The single phase nature of the final product was checked by powder x-ray-diffraction technique [curved position sensitive detector INEL CPS120 (Cu Kα)]. Single crystals of $\simeq 1$ mm^3 size were obtained

with the "flux growth" method by slowly cooling (2° per hour) a liquid of composition $Mn_{15}Te_{85}$ in the temperature range 873–773 K.

The ^{125}Te Mössbauer spectroscopy measurements (3/2 - 1/2, 35.6 keV transition) were performed using a sinusoidal drive motion of a $Mg_3{}^{125m}TeO_6$ source kept either at 4.2 K or at room temperature. The $MnTe_2$ absorber was maintained at different temperatures between 4.2 K and room temperature. An absorber thickness of about 50 mg of natural Te/cm^2 was used. The 35.6 keV γ rays were detected with an intrinsic Ge detector well suited to discern the intense Te Kα (27.5 keV) and Kβ (31.0 keV) x rays from the Mössbauer γ rays. The velocity calibration of the spectrometer was performed using a $^{57}Co/Rh$ source and a metallic iron absorber. The experimental data were directly analyzed by a least-squares method to obtain the hyperfine parameters by constraining the relative energies and intensities of the Lorentzian lines to theoretical values. In the case of combined quadrupole and magnetic interactions, the calculation of the spectral shape is performed by diagonalization of the full nuclear Hamiltonian. In that situation, the fitting routine provides the value of the transferred hyperfine field (H_{hf}), the isomer shift (δ_{IS}), the quadrupole coupling constants (eQV_{zz}, η), the relative orientation (θ, φ) of the field H_{hf} with respect to the z axis of the electric-field-gradient tensor (efg). This axis coincides with the local symmetry axis of each anion pair Te_2^{2-} which is along one of the four-body diagonal $\langle 111 \rangle$ directions.

The neutron experiments were carried out at the high flux reactor of the Institut Laue-Langevin (Grenoble). The powder experiment was performed on the 400 cells position-sensitive detector diffractometer D1B in the temperature range 45–150 K. The wavelength $\lambda=2.522$ Å was used and was provided by a focusing pyrolitic graphite monochromator. The sample was enclosed in a cylindrical vanadium container 5 mm in diameter and 5 cm in height. The analysis of the powder patterns was performed by Rietveld profile refinement using the software FULLPROF.[5] The experiment on the single-crystal specimen was conducted in two steps on the two-axis spectrometer D15, operating in the normal beam mode. The wavelength $\lambda=1.17$ Å was provided by a flat copper monochromator. In a first step, the crystal was mounted in a cryomagnet with its **c** axis roughly 10° from the ω axis of the spectrometer, this axis being the direction of the applied field. The orientation matrix was determined by centering a set of 15 reflections. Several peaks were then scanned while cooling down the sample (zero-field cooled). Then, the sample was heated up, and the same reflections were measured under the same temperature conditions, but in an applied field $H=4$ T (field cooled). This experiment was carried out to determine whether domains exist in the crystal. Then, in a second step, the crystal was mounted in a liquid-helium cryostat. The orientation matrix was determined from the same reflection set as before. Bragg intensities were then collected at three different temperatures (4.2, $\simeq 60$, and $\simeq 80$ K), in order to refine the magnetic structure. In both cases, integrated intensities were measured by rotating the crystal with the detector held in a fixed position. The integration of the peaks was done during experimental runtime using the COLL5N program.[6] The refinements of the data were carried out using the MXD package.[7] The scattering lengths
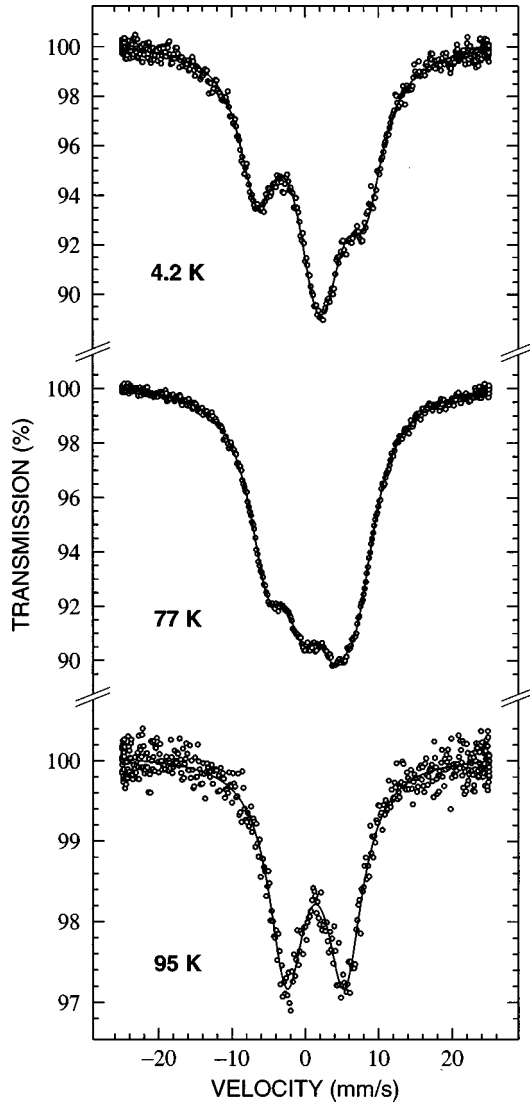
FIG. 3. ^{125}Te Mössbauer spectra at $T=4.2$, 77, and 95 K.

b_{Mn} and b_{Te} were taken from Koester et al.,[8] and the magnetic form factor of Mn from Brown.[9]

III. ^{125}Te MÖSSBAUER STUDY

A. Experimental results

The Mössbauer study had a double aim: (a) to check if the discontinuous changes of the transferred hyperfine and quadrupole coupling constant at 60 K as reported by Kasai et al.[4] is not an artifact of their fitting procedure, (b) to confirm the kind of magnetic ordering postulated by our single-crystal neutron experiments.

^{125}Te Mössbauer spectra recorded in the paramagnetic and magnetically ordered states are shown in Fig. 3. The Mössbauer data at $T>T_N$ are well represented by a quadrupole doublet whose splitting $\frac{1}{2}eQV_{zz}(1+\eta^2/3)^{1/2}=7.9(1)$ mm/s well agrees with published values.[2,4] The linewidth $W=5.9(2)$ mm/s at 95 K is close to the value expected for a thin absorber ($\simeq 5.6$ mm/s).[10] The isomer shift at 95 K with respect to the Mg$_3$TeO$_6$ source at room temperature is 1.35(6) mm/s.

The data recorded below T_N clearly show the presence of a magnetic hyperfine structure. This behavior provides evidence for the presence of a transferred hyperfine field at the tellurium nuclei due to the ordering of the Mn^{2+} sublattice. The 4.2 K spectrum can be analyzed satisfactorily on the basis of two quite different sets of hyperfine interaction parameters: (a) $H_{\text{hf}}=97(2)$ kG, $\frac{1}{2}eQV_{zz}=-8.2(1)$ mm/s, $\theta=16(2)°$; (b) $H_{\text{hf}}=124(2)$ kG, $\frac{1}{2}eQV_{zz}=-6.6(1)$ mm/s, $\theta=26(3)°$. The latter set is similar to that reported by Kasai et al.,[4] while the former is close to the results given by Pasternak and Spijhervet.[2] In both sets the asymmetry parameter (η) was fixed to zero, in agreement with the ^{129}I Mössbauer impurity measurements in MnTe$_2$.[11] The spectra recorded at higher temperatures were thus analyzed assuming an axially symmetric efg. Approximately above 60 K, only one set of parameters is able to reproduce the experimental data, e.g., at 77 K, $H_{\text{hf}}=62(2)$ kG, $\frac{1}{2}eQV_{zz}=-8.0(1)$ mm/s, $\theta=19(2)°$. It turns out that it is possible to fit the data over the entire magnetically ordered state with the assumption that the angle θ between H_{hf} and the efg principal axis is basically temperature independent ($\theta\simeq 18°$) and that the quadrupole splitting below and above T_N is almost identical. In the absence of any structural phase transition at low temperature, as shown by previous x-ray-diffraction data,[4] one does not expect, even for a minute change of the x_{Te} parameter, a drastic temperature dependence of the quadrupolar splitting which is mainly due to the imbalance of the population in the p orbitals of the Te atom of the Te$_2^{2-}$ anion pair. Furthermore, the transferred hyperfine field and the Mn ordered moment follow the same temperature dependence. It is concluded that there is no need to invoke a discontinuous change of H_{hf} and eQV_{zz} at 60 K resulting from a spin rearrangement. This conclusion is in full agreement with the ^{57}Fe: MnTe$_2$ Mössbauer study of Saeed Khan et al.[12]

B. Transferred hyperfine field and magnetic structure

Each Te atom ($5p^5$ electronic configuration) of the dumbbell-shaped Te$_2^{2-}$ anion pair is surrounded by three nearest-neighbor Mn^{2+} cations. The occurrence of covalency effects, i.e., electron transfer between the magnetic Mn^{2+} ions and the ligand is evidenced by the presence of a transferred hyperfine field at the Te site and by the observation of a reduced quadrupolar splitting ($\simeq -8$ mm/s) compared to the one estimated for a single hole in the $5p$ shell (-12 mm/s).[13] The hyperfine field transferred at the ligand arises mainly from an isotropic contribution provided by the finite spin density in the $5s$ valence orbital and from an anisotropic term due to an unpaired spin density transferred into the $5p$ valence orbital of Te.[14] When, as in our case, the magnetic ion is an S-state ion as for Mn^{2+} ($t_{2g}^3e_g^2$ configuration), it is expected that the anisotropic contribution should be small. Indeed, the spin density transferred from the $3d(t_{2g})$-π orbitals and $3d(e_g)$-σ orbitals are of comparable magnitude.[15] Thus, one could consider, at least in a first approximation, that the transferred hyperfine field is basically isotropic, i.e., that the direction of H_{hf} is collinear with the weighted vectorial sum of the three nearest-neighbor magnetic moments of the Te atoms. The orientation (θ) of H_{hf} with respect to the principal axis of the efg thus provides information on the actual magnetic structure of MnTe$_2$. A

collinear type-I arrangement of the Mn moments will always lead to two distinct θ angles unless the easy direction is along a cube edge, then $\theta = 54.7°$.[3] The collinear structure can safely be rejected because the experimental θ value is about 18° over the entire ordered state. The noncollinear models (b) and (c) lead both to a unique θ angle, but with quite different values, 35.3° and 0°, respectively. The experimental value ($\simeq 18°$) clearly deviates from these expected values. This indicates that although small, the anisotropic contribution to H_{hf} cannot be neglected. The magnetic structure of MnTe$_2$ is noncollinear but no definite conclusion can be drawn from Mössbauer spectroscopy about its exact nature ($\mu_{Mn} \| \langle 110 \rangle$ or $\mu_{Mn} \| \langle 111 \rangle$). The answer is provided by the single-crystal neutron diffraction in an applied field presented in the next section.

IV. NEUTRON-DIFFRACTION STUDY

A. Powder sample

The purity of the powder sample was checked by a preliminary pattern, recorded in the paramagnetic state, at $T = 150$ K. This pattern was refined using the already known crystallographic structure of MnTe$_2$. A very good agreement ($R_p = 1.87\%$, $R_{wp} = 2.72\%$) (Ref. 16) was obtained using the space group $Pa3$. The lattice constant was refined to $a = 6.9245$ (5) Å, while the x_{Te} positional parameter was found to be 0.3847 (4). The calculated line shape is Gaussian. Figure 4 shows the measured and calculated profile intensities obtained at this temperature.

The sample was then cooled to $T = 45$ K and a long duration pattern was recorded. This pattern (Fig. 4) is mainly characterized by the apparition of two additional peaks indexed as (100) and (110), and the increase of several nuclear contributions. It closely resembles that of Ref. 1. It was analyzed as previously carried out and a very good agreement was obtained ($R_p = 2.81\%$, $R_{wp} = 3.62\%$). The a parameter was refined to 6.9116(5) Å, x_{Te} to 0.3866(6), and the magnetic moment on each manganese atom was found to be $\mu_{Mn} = 4.17(4) \mu_B$.

Then several patterns were recorded with increasing temperature up to 120 K. These patterns were also analyzed by the Rietveld method. Figure 5 shows the variation of the magnetic moment and Fig. 6 the intensity ratio between the (100) and (110) magnetic Bragg peaks as a function of temperature.

As previously observed,[17] a strong diffuse scattering occurs around the (100) magnetic peak (Fig. 4). It appears far below the ordering temperature and persists over at much higher temperature. It can be seen on Fig. 4 that it is still present at $T = 150$ K. The width of this scattering is very large compared to Bragg reflections [$\simeq 5°$ full width at half maximum, compared to 0.35° for the (100) peak]. Moreover, its position is slightly shifted away from the position of the Bragg scattering ($2\theta \simeq 21.3°$ vs 20.94). This scattering has been attributed to an incommensurate phase with short-range order.[17] Our present results strongly support this conclusion.

B. Single crystal

Figure 7 shows the temperature variation of the four reflections (1 0 0), (0 1 0), (0 0 1), and (0 1 1) with and without
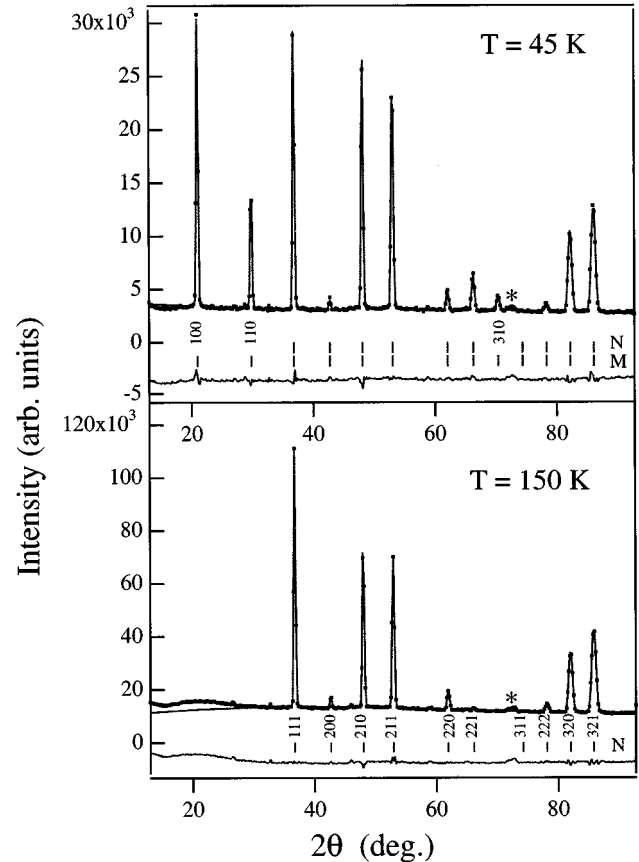
FIG. 4. Observed and calculated powder neutron-diffraction patterns at $T = 45$ K and $T = 150$ K as well as differences. The ticks indicate the positions of the reflections, for both the nuclear (N) and the magnetic (M) contributions. The weak peak marked with an * at $2\theta \simeq 72°$ is due to the vanadium sample holder.

applied field. The intensities of these four reflections do not depend on the applied field from T_N down to 4 K. One can then conclude that either there is only one domain in the crystal, or that there is no effect of the field on the domain structure. The three intensities (1 0 0), (0 1 0), (0 0 1) being equal, the second hypothesis would be that the three domains are exactly of the same size, whatever the cooling conditions and whatever the applied field. This second hypothesis is thus very unlikely, and both the collinear (model a) and the noncollinear model with $\mu_{Mn} \| \langle 110 \rangle$ (model b) can be reasonably excluded, to keep model c where $\mu_{Mn} \| \langle 111 \rangle$. In this model, the moments of the four manganese atoms of the unit cell point along the different diagonals of the cube which correspond to their local axes, to result in equivalent intensities for the three reflections (1 0 0), (0 1 0), and (0 0 1). This is the most natural arrangement of the magnetic moments in terms of symmetry, whereas in the two other models the symmetry of the different sites should be broken. The ratio between the (100) and (110) magnetic Bragg peaks being constant throughout the whole investigated range of temperature (Fig. 6), any rotation of the magnetic moments is excluded, and one can conclude that the nature of the magnetic structure stays the same at all temperature, as already evidenced from Mössbauer spectroscopy and from the powder neutron experiment.
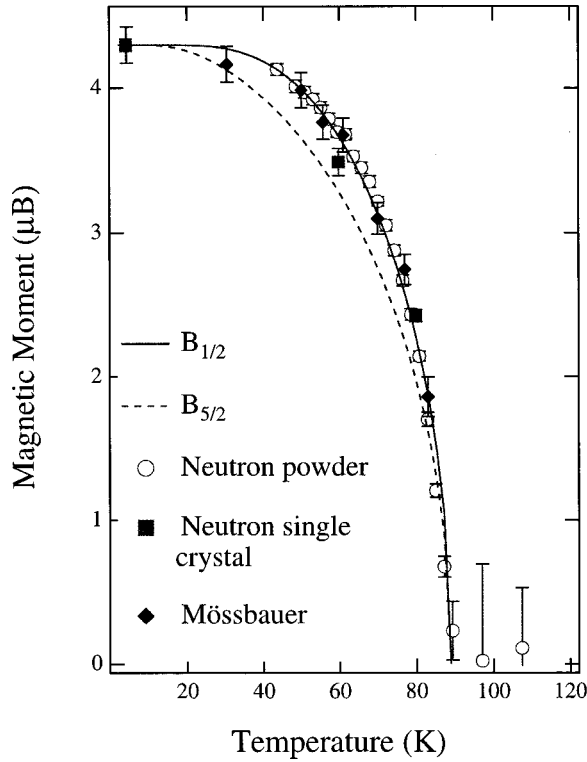
FIG. 5. Variation of the magnetic moment as a function of the temperature. The ^{125}Te hyperfine field measured at 4.2 K was scaled to the value obtained by neutron diffraction.

The intensities collected in the second part of the single-crystal experiment were then refined, considering this hypothesis (Table I). The 190 independent reflections measured at 4 K, the 97 reflections measured at 60 K, and the 171 reflections measured at 80 K were used to refine the magnetic moment amplitude, the x_{Te} coordinate of the tellurium atom, and a scale factor. A very good agreement value was obtained for the three data sets ($R_w = 4.10$, 3.98, and 3.92 %).[18] The refined parameters are given in Table II and are reported in Fig. 5. The continuous variation of the magnetic moment up to T_N shows the second-order nature of the
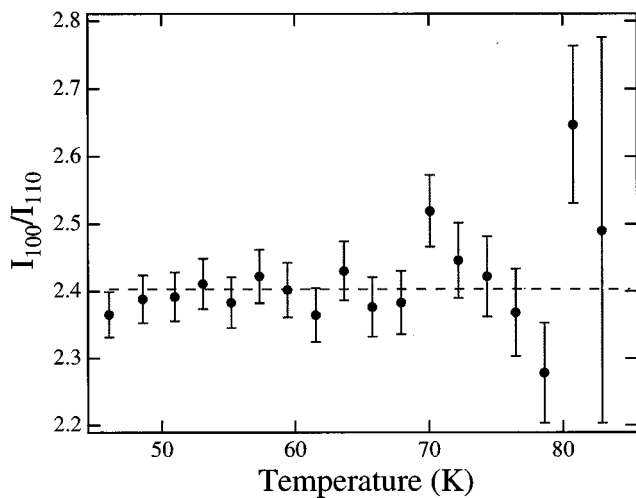
FIG. 6. Ratio of the intensities of the (1 0 0) and (1 1 0) reflections as a function of the temperature.
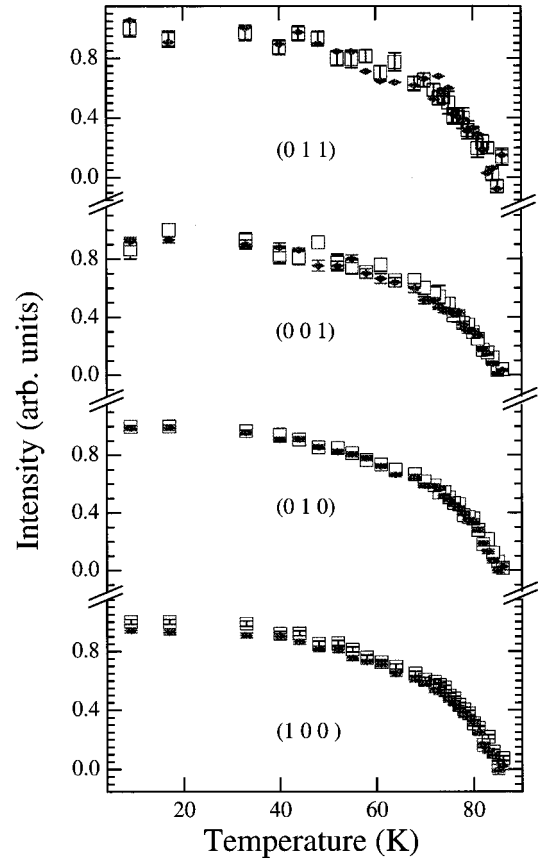
FIG. 7. Temperature variation of the (1 0 0), (0 1 0), (0 0 1), and (0 1 1) reflections in zero applied field (empty boxes) and in a field $H = 4$ T (full diamonds).

phase transition in MnTe$_2$. The values obtained from powder neutron diffraction, single-crystal neutron diffraction, and Mössbauer spectroscopy are in good accordance. We have reported in Fig. 5 the Brillouin curves $B_{5/2}$ and $B_{1/2}$ expected in a mean-field approximation. The experimental variation of the moment is sharper than the function $B_{5/2}$ expected, and surprisingly resembles the $B_{1/2}$ function. It is worth noting that the saturated manganese moment in MnTe$_2$ ($4.28\mu_B$, Table II) is significantly smaller than the expected free ion Mn^{2+} value of $5\mu_B$. The Mn^{2+} moment reduction ascribed to covalency effects and zero-point spin deviation compares well with that measured in MnTe ($4.27\mu_B$). This reduction is however larger than those observed in MnSe$_2$ ($4.39\mu_B$), α-MnS ($4.43\mu_B$), or MnO ($4.63\mu_B$).[19,20] This trend is in line with the expected increase in covalency from oxide to telluride. The x_{Te} parameter, as derived from the single-crystal experiment, is roughly constant in the whole range of

TABLE II. Results of the single-crystal data refinements.

	4 K	60 K	80 K
Moment (μ_B)	4.28(4)	3.46(9)	2.43(5)
x_{Te}	0.3847(3)	0.3849(3)	0.3851(3)
R_w (%)	4.10	3.98	3.92
χ^2	3.10	2.61	2.16

temperature (Table II). No drastic change occurs from a structural point of view with the onset of the magnetic ordering.

V. CONCLUSION

Our neutron-diffraction experiments and ^{125}Te Mössbauer study confirm that MnTe$_2$ orders antiferromagnetically in a noncollinear spin configuration. Additional details on the magnetic structure were provided by in-field single-crystal neutron experiments which strongly support the conclusion that the spins are parallel to the $\langle 111 \rangle$ axes of the threefold rotation symmetry. In contrast to previous claims,[2,4] this structure is stable down to 4.2 K. We find no indication of any spin rotation around 60 K and no anomaly of the x_{Te} positional parameter of the tellurium atom at that temperature.[4] According to recent work, the stabilization of a noncollinear spin structure as observed in MnTe$_2$ can be ascribed to anisotropic nearest-neighbor spin-spin exchange such as the Dzyaloshinsky-Moriya interaction.[21] We also pointed out that our data cannot be interpreted in terms of a purely ionic model. Covalency effects show up, not only in the observation of a spin density at the tellurium site, but also by a significant reduction of the quadrupolar interaction (Te) and of the ordered moment as compared to the values expected for free Te$_2^{2-}$ and Mn^{2+} ions.

[1] J. M. Hastings, N. Elliot, and L. M. Corliss, Phys. Rev. **115**, 13 (1959).

[2] M. Pasternak and A. L. Spijkervet, Phys. Rev. **181**, 574 (1969).

[3] J. M. Hastings, L. M. Corliss, M. Blume, and M. Pasternak, Phys. Rev. B **1**, 3209 (1970).

[4] N. Kasai, Y. Nishihara, and S. Ogawa, J. Phys. Soc. Jpn. **51**, 452 (1982).

[5] J. Rodriguez-Carvajal, Physica B **192**, 55 (1993).

[6] M. S. Lehmann and F. K. Larsen, Acta Crystallogr., Sect. B: Struct. Crystallogr. Cryst. Chem. **26**, 1198 (1970).

[7] P. Wolfers, J. Appl. Crystallogr. **23**, 554 (1990).

[8] L. Koester, H. Rauch, and E. Seymann, At. Data Nucl. Data Tables **49**, 65 (1991).

[9] P. J. Brown, in *International Tables for Crystallography*, edited by A. J. C. Wilson (Kluwer, Dordrecht, 1992), pp. 391–399.

[10] W. Bresser, M. Zhang, L. Koudelka, J. Wells, P. Boolchand, G. J. Ehrhart, and P. Miller, Phys. Rev. B **47**, 11 663 (1993).

[11] M. Pasternak, Phys. Rev. **184**, 523 (1969).

[12] M. A. Saeed Khan, V. H. Mc Cann, J. B. Ward, and R. J. Pollard, J. Phys. C **16**, 4011 (1983).

[13] R. M. Cheyne, C. H. W. Jones, and S. Husebye, Can. J. Chem. **53**, 1855 (1975).

[14] J. P. Sanchez, B. Djermouni, J. M. Friedt, and G. K. Shenoy, Hyperfine Interact. **1**, 313 (1976); J. M. Friedt, J. P. Sanchez, and G. K. Shenoy, J. Chem. Phys. **65**, 5093 (1976).

[15] J. P. Sanchez, J. M. Friedt, B. Djermouni, and G. Jehanno, J. Phys. Chem. Solids **40**, 585 (1979).

[16] R_p and R_{wp} are the standard Rietveld agreement factors defined as follows: $R_p = \Sigma_i |y_{obs}^i - y_{cal}^i| / \Sigma_i y_{obs}^i$ and $R_{wp} = \sqrt{\Sigma_i w_i (y_{obs}^i - y_{cal}^i)^2 / \Sigma_i w_i (y_{obs}^i)^2}$.

[17] T. Chattopadhyay and H. Fjellvag, Phys. Lett. A **120**, 44 (1987).

[18] R_w is the crystallographic weighted R factor: $R_w = \Sigma_i^{Nobs} w_i |G_{obs}^i - G_{cal}^i| / \Sigma_i^{Nobs} w_i |G_{obs}^i|$ where G_{obs} is the square root of the intensity (absolute value of the structure factor).

[19] A. J. Jacobson and B. E. F. Fender, J. Chem. Phys. **52**, 4563 (1970).

[20] B. C. Tofield, in *Structure and Bonding* (Springer-Verlag, Berlin, 1975), Vol. 2, p. 1.

[21] M. T. Heimilä and A. S. Oja, Phys. Rev. B **49**, 11 995 (1994).